Building and Environment 94 (2015) 859–866

Contents lists available at ScienceDirect

Building and Environment

journal homepage: www.elsevier.com/locate/buildenv

Inverse estimation of the non-acoustical parameters of loose granular absorbers by Simulated Annealing

Pedro Cobo [a, *], Elcione Moraes [b], Francisco Simón [a]

[a] Institute of Physical and Information Technologies (ITEFI), CSIC, Serrano 144, 28006 Madrid, Spain
[b] Faculdade de Arquitetura e Urbanismo, ITEC/UFPA, Tv. Augusto Corrèa, 01. 66075-110, Belém/PA, Brazil

ARTICLE INFO

Article history:
Received 17 March 2015
Received in revised form
29 April 2015
Accepted 1 May 2015
Available online 19 May 2015

Keywords:
Sound absorption
Loose granular materials
Simulated Annealing
Non-acoustical parameters

ABSTRACT

Absorbing materials are fundamental for the acoustic design of buildings. They are used for increasing the insulation from either outdoor or neighbour noise and for raising the acoustic comfort of dwellings. If environmental and health issues are not of concern, conventional sound absorbers, namely synthetic foams and fibrous materials, offer an excellent acoustical performance at a moderate cost. However, the current trend towards eco-efficient products encourages the enhanced use of natural fibre and loose granular recycled materials. Whatever the material type, a model is required to reliably predict its acoustical performance. The microstructural Champoux–Stinson model has demonstrated to provide consistent acoustical predictions once five non-acoustical parameters are given. Instead of measuring these non-acoustical parameters, which is a rather sophisticated and time consuming procedure, an inverse method, based on Simulated Annealing, is proposed in this paper to estimate them from a single and simple measurement of the absorption coefficient. Experimental results on two samples of loose aquarium gravel validate the proposed inverse method.

1. Introduction

The correct design of houses should combine the five essentials of buildings: structure, design, lighting, heating, and acoustics [1]. Acoustic design of houses has to do with their geometry (Room Acoustics) and with the use of acoustical materials (both absorbing and insulating) as a noise and reverberation control tool inside dwellings (Building Acoustics).

Sound absorbing materials are used in buildings mainly to increase the transmission loss across multilayer walls, to decrease the reverberation in enclosures, or to attenuate noise produced by internal sources. The combined use of insulating/absorbing materials allows designing lighter sandwich structures for attenuate noise incoming from outside sources (road, air or rail traffic, mainly). Excessively reverberant spaces, like restaurants, railway stations or airport rooms, reduce the speech intelligibility making difficult the communication. In noise control applications, the objective is to reduce sound levels to prevent harmful effects such as hearing damage and annoyance.

Sound absorption dissipates sound energy into heat by viscous and thermal effects [2–4]. Most of sound absorbing materials are porous-type, resonator-type or mixed porous-resonator type. Porous-type absorbers consist of two phases: a solid (rigid or flexible) skeleton and air in between. Sound absorption in porous materials is produced by the particle velocity and thermal gradient between the solid and gas phases of the material. Resonators, in the other hand, consist of a large volume with a small aperture, where the viscous-thermal dissipative effects are produced. According to Arenas and Crocker [5], based on their microstructural configuration, porous absorbing materials can be classified as cellular, fibrous or granular. They can be modelled as cubic cells with connecting pores, parallel fibre bundles, or stacked identical spheres, respectively. Examples of these materials are foams (cellular), mineral wools (fibrous), and gravels or sands (granular).

The most used sound absorbing materials in buildings are synthetic foams and fibrous materials. If environmental and health issues are not of concern, they offer an excellent acoustical performance at a moderate cost. However, the manufacture of synthetic absorbing materials increases the emission of greenhouse gases into the atmosphere, and therefore may affect the carbon footprint of industrialized countries [5]. Thus, as the concept of green building materials is being introduced in these countries, there is a need for the search of more environmentally friendly

* Corresponding author. Tel.: +34 91 5618806; fax: +34 91 4117856.
E-mail address: pedro.cobo@csic.es (P. Cobo).

http://dx.doi.org/10.1016/j.buildenv.2015.05.009
0360-1323/

materials. A clear example of this trend is the proposal of natural fibre and recycled materials [6]. Many of these recycled materials are of the granular type and may come from the waste generated in other production plants, which encourage the launching of eco-efficient products [7].

Whatever the material type, a model is needed to predict the acoustical performance of sound absorbers. A sound absorption model relates acoustical variables of the material, such as propagation constant and characteristic wave impedance, to non-acoustical parameters. The sound absorption coefficient, either at normal, oblique or random incidence, of an absorbing layer can be predicted from these acoustical variables. The number of non-acoustical parameters needed depends on the refinement grade of the model. Absorption models are of the empirical, phenomenological or microstructural types. Voronina and Horoshenkov [8] proposed an empirical absorption model that depends on four non-acoustical parameters (porosity, tortuosity, specific density of the grain base, and characteristic dimension of particles), and have been applied to loose granular materials. Currently, however, more sophisticated phenomenological and microstructural models have been proposed [9]. For instance, the phenomenological Hamet–Berengier model requires three non-acoustical parameters (flow resistivity, porosity, and tortuosity) and is the most accepted model to predict the acoustical behaviour of pavements [10]. In this paper, however, the microstructural model proposed by Champoux and Stinson [11], which is based on five non-acoustical parameters (flow resistivity, porosity, and tortuosity, viscous pore shape factor, and thermal pore shape factor), is preferably used.

In a normal use of a sound absorbing model (direct modelling), the non-acoustical parameters should be first measured and then entered into the propagation constant and characteristic acoustic impedance equations to obtain its sound absorption curve as a function of the frequency. However, instead of measuring these non-acoustical parameters of absorbing materials, inverse strategies can be applied to calculate them once the sound absorption at normal incidence has been experimentally evaluated [12,13]. This inverse approach requires the assumption of a material absorption model and an optimisation algorithm. The objective of the optimisation algorithm is to obtain the non-acoustical parameters that minimize the difference between the measured and modelled absorption curves. Some authors have used a microstructural model combined with genetic [12,13], non-lineal best fitting algorithms [13], or sequential linear programming [14], to estimate the five non-acoustical parameters of porous fibrous materials. Others, have used impedance models for graded cellular metals [15] or multilayered microperforated panels [16] combined with simulating annealing algorithms to maximise the mean absorption within a prescribed frequency band.

The main aim of this paper is to illustrate the inverse method of determining the non-acoustical parameters of a sound absorbing granular material by combining the Champoux and Stinson (CS in the following) absorption model with the simulating annealing optimisation algorithm (SA in the following). The CS model and the SA algorithm are reviewed first in Sections 2 and 3, respectively. Section 4 describes in more detail the granular absorber, the measurement of its non-acoustical parameters and absorption coefficient, and the estimation of some of its non-acoustical parameters by SA. Finally, the main conclusions of this study are outlined in Section 5.

2. The CS model for porous absorbers

The input acoustic impedance to an absorbing layer of thickness d backed by a rigid wall is [9]

$$Z_i(\omega) = Z_s \ \coth[-ik_s d], \tag{1}$$

where Z_s is the complex characteristic acoustic impedance and k_s the complex wave number of the absorbing material. Once the input acoustic impedance, Z_i, is known, the normal incidence reflection, R, and absorption, α_0, coefficients can be calculated from

$$R = \frac{Z_i - Z_0}{Z_i + Z_0}, \tag{2}$$

$$\alpha_0 = 1 - |R|^2, \tag{3}$$

where Z_0 is the air characteristic impedance. Champoux and Stinson [11] proposed a microstructural model that depends on the five non-acoustical parameters (σ,ϕ,q,s_p,s_k), where σ is the flow resistivity, ϕ is the porosity, q is the tortuosity, and s_p and s_k are the viscous and thermal pore shape factors, respectively. The CS model is based on the following equations for the complex dynamic density, ρ_g and the complex dynamic bulk modulus, K_g,

$$\rho_g(\omega) = \rho_0 q^2 - i\frac{\sigma\phi F(\lambda_p)}{\omega}, \tag{4}$$

$$K_g(\omega) = \frac{\gamma P_0}{1 + \frac{2(\gamma-1)T(\Lambda_k)}{\Lambda_k}}, \tag{5}$$

where

$$F(\lambda_p) = -\frac{1}{4}\frac{\lambda_p\sqrt{-i}T\left(\lambda_p\sqrt{-i}\right)}{1 - 2\frac{T(\lambda_p\sqrt{-i})}{\lambda_p\sqrt{-i}}}, \tag{6}$$

$$\lambda_p = s_p\left[\frac{8q^2\rho_0\omega}{\sigma\phi}\right]^{1/2}, \tag{7}$$

$$\Lambda_k = \lambda_k\sqrt{-N_{Pr}i}, \tag{8}$$

$$\lambda_k = s_k\left[\frac{8q^2\rho_0\omega}{\sigma\phi}\right]^{1/2}, \tag{9}$$

and

$$T(\xi) = \frac{J_1(\xi)}{J_0(\xi)}, \tag{10}$$

being J_o and J_1 the zero and first Bessel functions, respectively, ρ_0 the air density, γ the air specific heat ratio, N_{Pr} the air Prandtl number, and P_0 the ambient atmospheric pressure. Once ρ_g and K_g are known, the characteristic impedance, Z_s, and the wave number, k_s, are calculated by

$$Z_s = \frac{1}{\phi}[\rho_g K_g]^{1/2}, \tag{11}$$

$$k_s = -\omega[\rho_g/K_g]^{1/2}. \tag{12}$$

Making use of the non-acoustical parameters (σ,ϕ,q,s_p,s_k) into Eqs. (4)–(12) a complete model is obtained that predicts the acoustical properties (Z_s,k_s) of the porous material, which can be introduced into Eqs. (1)–(3), once the layer thickness d is specified, to calculate the sound absorption coefficient of the sample.

3. Optimization by SA

The problem of finding the set of non-acoustical parameters $(\sigma,\phi,q,s_p,s_k,d)$ that minimizes the difference between the measured and theoretical absorption curves can be posed as a global optimization problem. To illustrate the problem, Fig. 1 shows the function

$$F(\alpha_m) = \sum_n \left|\alpha_{Meas}(f_n) - \alpha_{CS,m}(f_n)\right|, \tag{13}$$

where f_n is a discrete frequency within the range of optimization, $\alpha_{Meas}(f_n)$ is the measured absorption curve of a granular sample and $\alpha_{CS,m}(f_n)$ is the theoretical absorption curve provided by the CS model for the combination of non-acoustical parameters $(\sigma_m,\phi_m,q_m,s_{pm},s_{km},d_m)$ within the range

$$\begin{aligned} \sigma_m &\in [1000, 10000]\ \mathrm{Pa\cdot s\cdot m^{-2}} \\ \phi_m &\in [0.1, 0.8] \\ q_m &\in [1.1, 1.9] \\ s_{pm} &\in [1.0, 1.6] \\ s_{km} &\in [0.4, 1.0] \\ d_m &\in [1.0, 15]\ \mathrm{cm} \end{aligned} \tag{14}$$

In general, the non-acoustical parameters vary continuously within their ranges. However, for the problem can be solved by exhaustive search, each of them has been discretized in ten values. Even though the number of configurations has been chosen purposely low (1 million in this case), so that the problem can be solved by exhaustive search, the code programmed in a PC with Intel Core i3 spent almost 21 h to find the solution. Two features of the objective function call the attention: the spiky nature of the $F(\alpha_m)$ function, with many alternate local minima and maxima, and the variety of non-acoustical parameters which provide very similar values of the $F(\alpha_m)$ function. The challenge of any optimization algorithm is to find the global minimum avoiding be trapped in one of the many local minima. Simulated Annealing (SA) is an optimization method especially appropriate for these types of problems [17].

SA is a numerical method inspired in a process, called annealing, occurring in nature. In metallurgy, for instance, annealing alters the microstructure of a material producing changes in properties such as strength, hardness and ductility. When the metals are slowly cooled from a high temperature state, atoms rearrange themselves to reach minimum energy following the Boltzmann law [16]. Let ΔE be the energy change from one state to another at a temperature T. The Boltzmann law establishes that the probability that the system change from one state to another is

$$Pr\{E\} = \frac{1}{C(T)}\exp\left\{-\frac{\Delta E}{K_B T}\right\}, \tag{15}$$

where $C(T)$ is a normalization factor and K_B is the Boltzmann constant. Thus, when the temperature is high, there is a high probability to accept a new state with a higher energy. However, as the temperature decreases states with higher energy are more improbable, and eventually, when the temperature approaches to zero, only minimum energy state will likely be accepted. In this process, slow cooling is essential, allowing ample time for redistribution of atoms as they lose mobility.

SA optimization of functions exploits the analogy with this natural annealing process. The application of the Boltzmann scheme to the function optimization problem is named the Metropolis algorithm [18]. To apply this algorithm to the optimization of a function is necessary to provide the following: (a) an objective function, analogous to the energy in natural annealing; (b) a space of configurations, similar to the states in metals; (c) a random mechanism to change for one configuration to another; (d) a control parameter T, analogous to the temperature in natural annealing, and (e) a cooling schedule that establishes the decreasing velocity of T.

In this work, the objective function to be minimized is the sum of the absolute difference between measured and theoretical absorption curves $F(\alpha_m)$ defined by Eq. (13). The space of configurations consists of combinations of the non-acoustical parameters $(\sigma_m,\phi_m,q_m,s_{pm},s_{km},d_m)$ within the range defined by Eq. (14). To pass from one configuration to another, only one parameter is changed

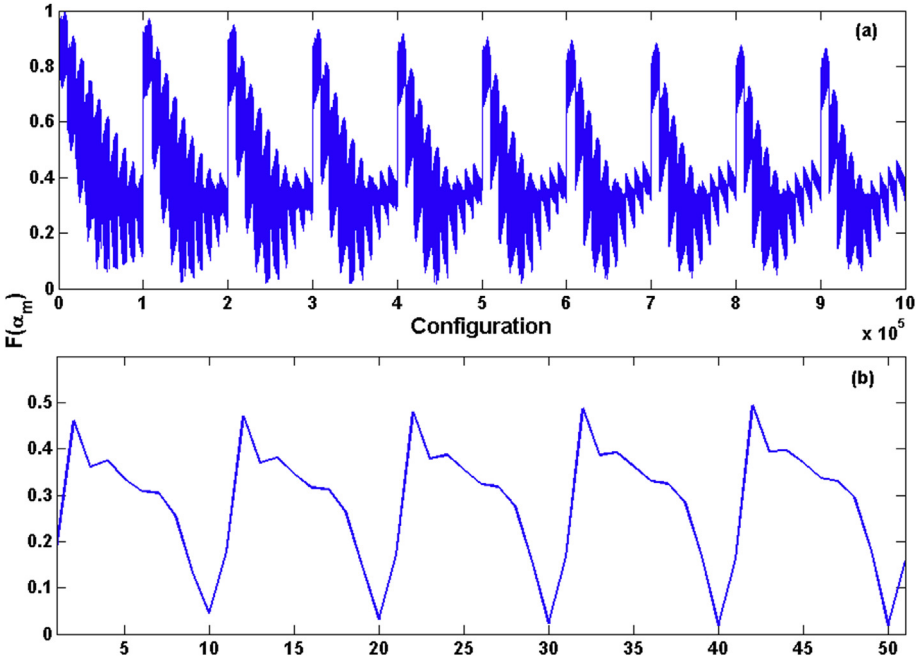

Fig. 1. (a) Evolution of the objective function $F(\alpha_m)$ with the configuration number for the case of exhaustive search. (b) A zoom around the minimum of $F(\alpha_m)$.

randomly, this ensuring that both configurations are in the vicinity of each other. To implement the Metropolis algorithm, a $\Delta F = F(\alpha_m)_{new} - F(\alpha_m)_{old}$ factor is defined for a new configuration at temperature T. The new configuration is accepted whether $\Delta F < 0$ or $Pr(T) = \exp(-\Delta F/T) > \varphi$, being φ a random number in the interval [0,1]. Therefore, configurations with lesser values of the objective function are accepted unconditionally, whilst configurations with larger values of the objective function are accepted only if the corresponding Boltzmann factor is larger than φ. This mechanism of choosing always configurations with $\Delta F < 0$ but sometimes configurations with $\Delta F > 0$ prevents the objective function from being trapped in a local minimum.

The cooling schedule includes the initial temperature, T_{ini}, the final temperature, T_{fin}, and the cooling velocity geometrical law [19,20].

$$T_{k+1} = \zeta T_k, \tag{16}$$

with the cooling factor $0 < \zeta < 1$. The algorithm proceeds from T_k to T_{k+1} when a number of iterations are attained. The process finalizes either when the final temperature, T_{fin}, is completed or when a number of changes are done without success in finding a better configuration.

4. Results

Loose aquarium gravel has been used as a sample of cheap and effective sound absorber. It was sieved to obtain a material with grain size between 3 and 4 mm. Once obtained a homogeneous sample, it was subjected to a series of tests to characterize its non-acoustical properties (ϕ, q, σ), which, in turn, will be used as a reference for the results of the method proposed in this work. The absorption coefficient was measured as well since it is the input parameter of the method. Later, the estimation of the non-acoustical parameters by SA is carried out. Finally the agreement degree of the measured and estimated by SA is analyzed.

4.1. Measurement of the non-acoustical parameters

4.1.1. Porosity determination

Porous materials useful in acoustics as absorbers are made up of a non-compact air-saturated solid frame. In the case of granular material, the frame is composed of grains that lean to each other. The fluid within the material makes interconnected open bubbles that allow the air to circulate all around the frame. A measurement of this property is the porosity, ϕ, defined as the ratio of the air volume inside the material, V_a, to the total volume of the porous material, V_T

$$\phi = \frac{V_a}{V_T}. \tag{17}$$

As $V_T = V_a + V_g$, ϕ can be expressed as a function of the densities of both the grain, ρ_g, and the material, ρ_m

$$\phi = 1 - \frac{\rho_m}{\rho_g}. \tag{18}$$

The measurement procedure used in this work is the so-called "vacuum impregnation" widely used in geophysical works [21]. According to this procedure, a known volume, V_T, of granular material is submerged in a liquid, and then it is introduced into a vacuum chamber, so that all the gas diluted in the liquid and all the remaining air bubbles within the pores, due to its surface pressure, are removed. This way the volume of liquid equals the volume of the open pores and V_a is obtained. V_t and V_a are then introduced in Eq. (17), and ϕ is determined.

This method is only valid for grains non-impervious to the water. Otherwise, another method should be used as those suggested by Champoux et al. [22], or [23,24] for very small pores.

4.1.2. Tortuosity determination

Another important microstructural parameter that helps to describe a porous material is the tortuosity, which is related with the orientation from the normal to the surface of the channels that make the pores together with the path that the acoustic wave has to follow to propagate within the material. The result is an increase of the distance of any acoustic path across the material. Zwikker and Kosten [25] introduced first this quantity. Lately, other authors have revised their model to take into account the nature of the porous skeleton of different types of porous materials. For example, Johnson related the tortuosity with the geometry of the pores and Allard showed that it is related with the kinetic energy of the wave in the pores.

The method used in this work to measure q is based on an electrical analogy [26]. If the porous material is immersed in an electrolyte solution, the path the ions have to go over is roughly the same than the path gone over by the acoustic field across the porous material. According to Allard et al. [27], a very important issue to take into account in this procedure is the presence of gas diluted in the liquid that changes significantly its conductivity. To prevent this problem, a vacuum chamber was used. In this way, q can be expressed as

$$q = \sqrt{\phi \frac{\varsigma_c}{\varsigma_f}}, \tag{19}$$

being ς_c and ς_f the resistivities of the saturated material and the fluid, respectively. As

$$\varsigma_i = R_i \frac{A_i}{d_i}, \tag{20}$$

where R_i is the electrical resistance, A_i is the surface of the electrodes, and d_i is its distance. Assuming that $A_c = A_f$ and $d_c = d_f$, then

$$q = \sqrt{\phi \frac{R_c}{R_f}}, \tag{21}$$

where R_i can be obtained by the Ohm's law. Fig. 2 shows the voltage measured for different electrical currents applied to the saturated

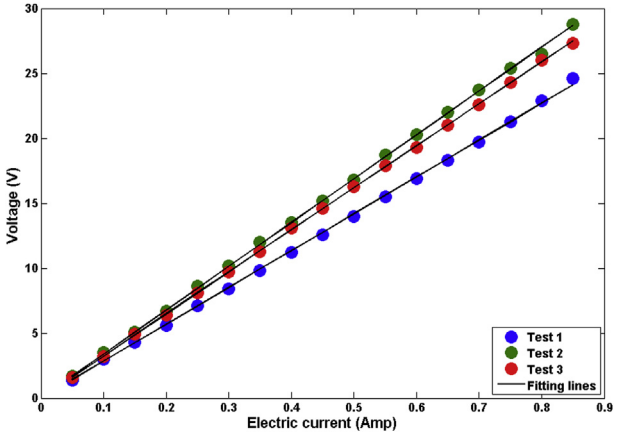

Fig. 2. Measurement of the electrical resistance of three different samples of gravel saturated with a conductive solution.

material placed between two electrodes. According to the Ohm's law, the slope of the straight lines is the resistance of the sample.

4.1.3. Flow resistivity determination

The flow resistivity quantifies the resistance of a porous material to be passed across by an airflow. This quantity is one of the main parameters related to the acoustical behaviour of porous materials and it is present in most of the models that describe the sound absorption of this type of materials. Flow resistivity, σ, can be defined as

$$\sigma = -\frac{\Delta P}{\Phi}\frac{A}{d}, \tag{22}$$

where ΔP is the air pressure difference across the porous layer, Φ is the mean flow of air, A is the cross-sectional area of the layer, and d is the thickness.

The method to measure the flow resistivity is standardized [28] and is based on a previous work by Bies and Hansen [29]. This method consists on passing a flow of air across a sample of a porous layer of known A and d, so that σ is determined using Eq. (22) once Φ and ΔP have been measured.

4.1.4. Results of the determination of the non-acoustical quantities

A series of measurements were carried out according to the methods described above. A total of five tests were done for each quantity (ϕ, q, and σ) on the two different samples with thicknesses 5 and 10 cm. Table 1 summarizes the results of the measurements of these non-acoustical parameters. Uncertainty values calculated for a 95% confidence level are also provided for the measured values. These results will then be compared with those estimated by SA to assess its quality.

4.2. Measurements of the absorption curves

Two samples of the sieved aquarium gravel, with nominal thicknesses $d = 5$ cm and $d = 10$ cm, were prepared to be measured in a Brüel&Kjaer 4206 impedance tube using the standard ISO10534-2 [30]. The transfer function between two Brüel&Kjaer 4187 microphones separated 2 cm was used to calculate the normal incidence sound absorption coefficient of the samples mounted at one end of the tube with inner diameter 29 mm (see Fig. 3), in the frequency range from 100 Hz to 6500 Hz.

Fig. 4 shows the normal incidence sound absorption coefficients of both samples as a function of frequency. A series of 5 tests were carried out and the uncertainty of the measurement estimated. Dash lines in Fig. 4 shows the upper and lower limits of the 95% confidence interval of the results. In general the average uncertainties are 0.016 and 0.024 for the samples of 5 and 10 cm respectively.

4.3. Estimation by SA of the non-acoustical parameters

4.3.1. Sensitivity analysis of the acoustic absorption model

A sensitivity analysis gives information on how the spread of every input parameter of a model can influence the span of the output. Traditionally, local sensitivity analysis is used when dealing with inverse problems. This type of study, based on partial derivatives all over the model, provides useful criteria to assess the uniqueness of the solution of an inverse problem and it is helpful for developing regularization strategies. Nevertheless, these techniques are inefficient in terms of analyst's time and even derivative are not always easy to obtain. In addition, when the inverse method is based on stochastic processes (as it is our case here), where it is important to obtain information of the whole space of the input parameters and not only of the base calculation point, local sensitivity becomes somewhat cumbersome. In these cases, global sensitivity analysis is a better option. It explores the whole input

Table 1
Non-acoustical parameters for the loose granular sample.

Parameter	Measured value
Flow resistivity, σ (Pa s m^{-2})	4850 ± 626
Tortuosity, q	1.36 ± 0.17
Porosity (ϕ)	0.434 ± 0.024
Layer thickness, d (cm)	{5, 10} ± 0.2

Fig. 3. Measurement rig for the sound absorption coefficient.

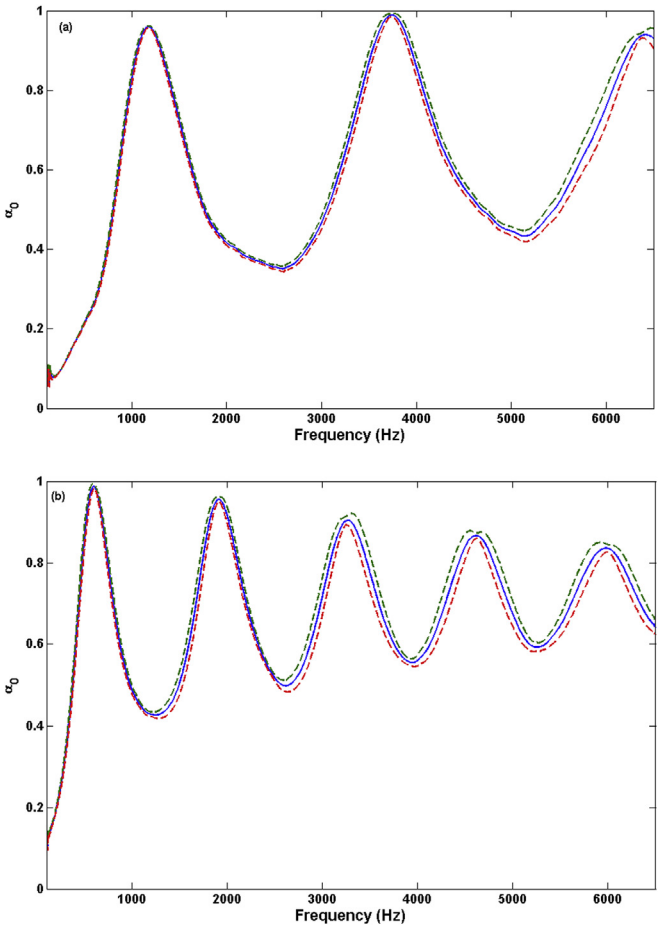

Fig. 4. Measured absorption curves of the granular absorber for the two samples of thicknesses (a) 5 cm and (b) 10 cm.

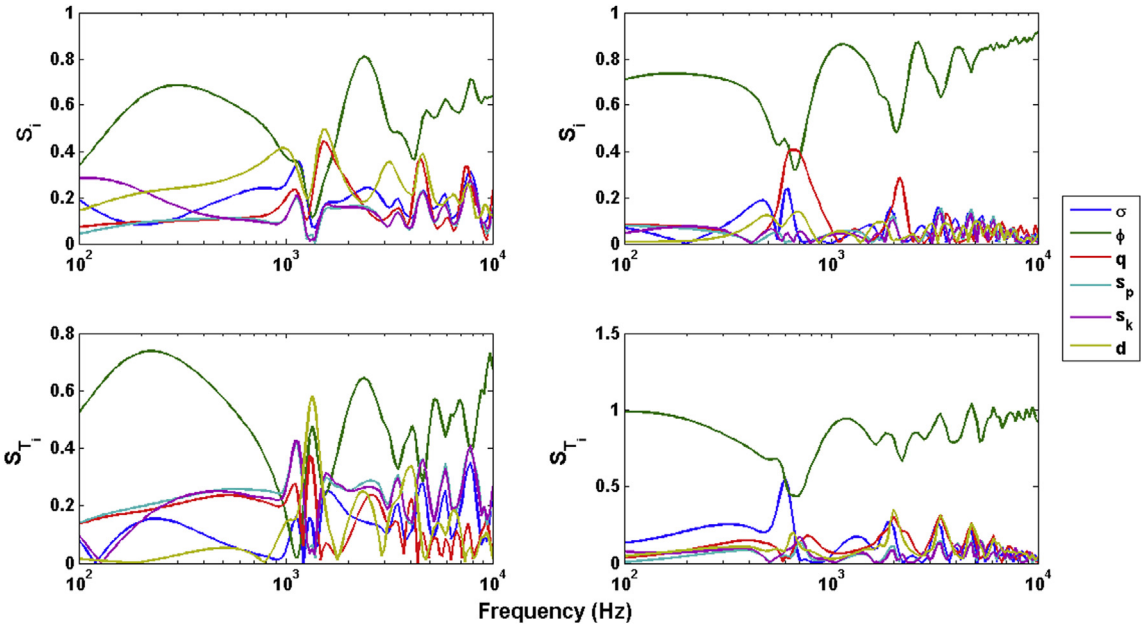

Fig. 5. First order (above) and total effect (below) sensitivity indices for the 5 cm (left) and 10 cm (right) samples.

space and gives information on how variance of each of the input parameters acts on the output variability.

Here a variance based sensitivity analysis method is used. It is based on the work of Saltelli et al. [31], which, in turn, is based on the Sobol's index [32]. It uses the first order and the total sensitivity indices.

The first order sensitivity index, S_i, is a measure of the importance of a given input parameter on the output and it can be expressed as

$$S_i = \frac{V_{X_i}\left(E_{X_{\tilde{i}}}(Y|X_i)\right)}{V(Y)}, \tag{23}$$

where $V_{X_i}(\cdot)$ is the variance over all possible values of X_i, $E_{X_{\tilde{i}}}(\cdot)$ is the expected value of Y for a fixed value of X_i ($X_{\tilde{i}}$), and $V(Y)$ is the variance of Y. Here a model $Y(X_i)$ has been assumed (in our case $\alpha(\sigma,\phi,q,d,s_p,s_k)$.

The total effect sensitivity index is typically used to identify non-influential input parameters and it is a measure of the overall effect of an input parameter on the output. It corresponds to the expected variance that is left when all inputs except for itself are fixed

$$S_{T_i} = \frac{E_{X_{\tilde{i}}}\left(V_{X_i}\left(Y|X_{\tilde{i}}\right)\right)}{V(Y)}. \tag{24}$$

Fig. 5 shows the first order and total effect indices for the CS model and for samples of 5 and 10 cm, respectively. Notice that the most important parameter is ϕ, especially for the 10 cm layer. In the 5 cm sample, d plays a role for frequencies under 2 kHz, but there exist certain interaction among the different input parameters. On the other hand, for the 10 cm sample, σ and q also has an influence on the results around 700 Hz. At high frequencies the model used is low sensitive to the spread of the rest of the parameters.

A conclusion of this study is that the SA method should be used with samples as thicker as possible and that initial conditions of porosity should be carefully chosen.

4.3.2. SA results

To demonstrate the capability of SA to estimate the non-acoustical parameters of the granular samples, the objective function $F(\alpha_m)$ defined in Eq. (13) is used in this Section, with α_{Mes} the measured absorption curves shown in Fig. 5 and α_{CS} the theoretical absorption curves provided by the CS model for each $(\sigma_m,\phi_m,q_m,s_{pm},s_{km},d_m)$ combination. In this Section the parameters vary continuously so that the problem cannot be solved by exhaustive search. In the following, the SA algorithm described in Section 3 is used, with $T_{ini} = 1$, $T_{fin} = 10^{-6}$, and $\zeta = 0.95$. The algorithm finalizes either when the final temperature is completed or when 50 changes of parameters are done without success in finding a better configuration.

To illustrate the functioning of the SA algorithm, the evolution of the temperature and objective function is shown in Fig. 6 for a case. At the beginning, when the temperature is still high, there is a high probability to accept successful configurations with higher values

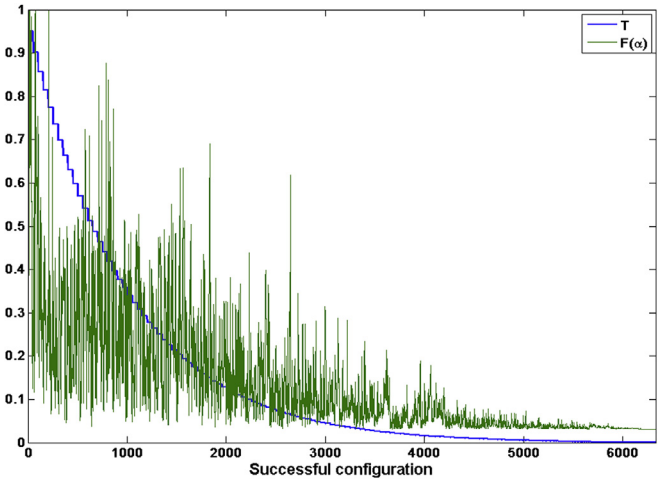

Fig. 6. Evolution of the temperature and objective function in the estimation of the non-acoustical parameters by SA.

Table 2
Measured and estimated by SA non-acoustical parameters for the $d = 5$ cm sample.

Parameter	Measured	Estimated		Relative error (%)	
		$d = 5$ cm	$d = 10$ cm	$d = 5$ cm	$d = 10$ cm
Flow resistivity, σ (Pa s m^{-2})	4850 ± 626	4539	4501	6.4	7.2
Porosity, ϕ	0.434 ± 0.024	0.41	0.39	4.6	9.3
Tortuosity, q	1.36 ± 0.17	1.59	1.48	18.6	10.4
Viscous pore shape factor, s_p	NA	1.34	1.2	NA	NA
Thermal pore shape factor, s_k	NA	0.83	0.9	NA	NA
Layer thickness, d (cm)	5 ± 0.2 or 10 ± 0.2	5.0	10.0	0	0

of the objective function. This probability, however, decreases as the temperature cools, and eventually, when the temperature is very low, only configurations with lesser values of the objective functions are accepted. This is the way as SA finds the global minimum value of the objective function without be trapped in a local minimum.

Table 2 summarizes the results of estimating the non-acoustical parameters by SA of the two samples of nominal thicknesses $d = 5$ cm and $d = 10$ cm. Each estimated value of the non-acoustical parameters is the average of 5 runs of the SA algorithm. The average time spent by the algorithm to find a solution was 23 min. Since the parameters values are intrinsic to the granular sample, and not to its thickness, the estimates in third and fourth columns of Table 2 should be close to each other. This is the case for (σ,ϕ) which estimations are rather consistent for both thicknesses, and are also within the range of validity of the measured values. This is also true for the estimation of d, the thickness of the two measured samples. On the other hand, more deviations are found between the values of (q,s_p,s_k) parameters provided by SA for each sample. Even in the case of q, the estimated values are also within the confidence interval of the measured value.

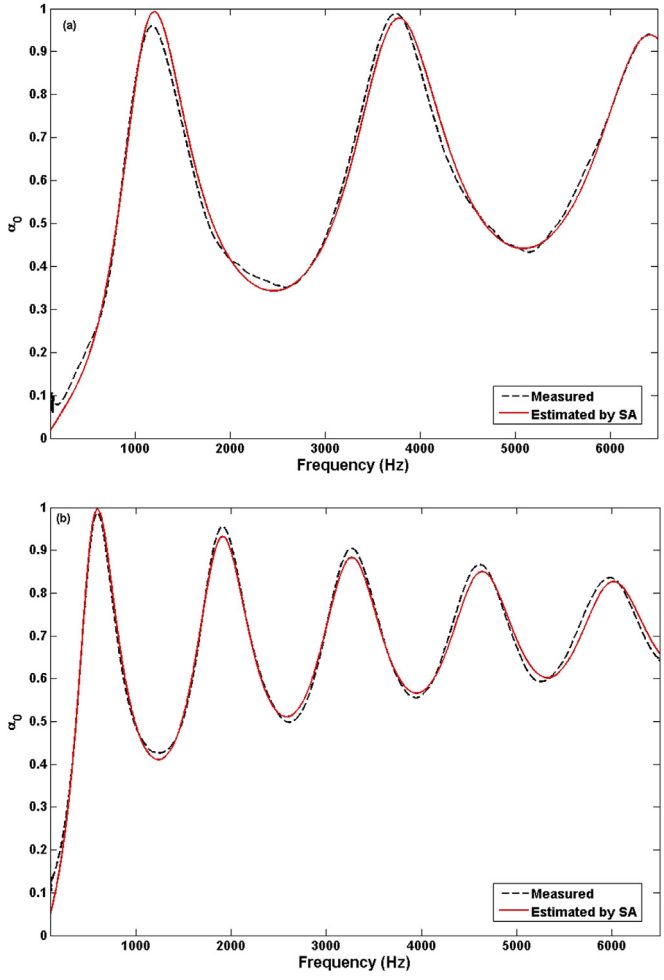

Fig. 7. Measured y estimated by SA sound absorption curves for the sample with (a) $d = 5$ cm and (b) $d = 10$ cm.

The remaining parameters (s_p,s_k) were not measured, so that they cannot be compared with the estimations by SA. However, it is known that they do not affect too seriously the predictions of the CS model [10]. Notice that if the averages of the two estimations are taken, then $\widehat{s}_p = 1.27$, and $\widehat{s}_k = 0.87$, which are expected values for granular absorbers [10].

The normal incidence sound absorption curves corresponding to these combinations of parameters are shown in Fig. 7. For the sake of comparison, the measured sound absorption curves are superimposed with the estimated by SA. The good concordance of both curves demonstrates the suitability of CS model to describe the acoustical performance of this loose granular material.

5. Conclusions

As it has been stated, a main way to design and control acoustic environment inside a building is by the use of acoustic materials useful to rule indoor acoustics or even improve the performances of multilayer building elements used in acoustic insulation. Currently, as the concept of green eco-efficient building materials is being introduced, which in addition need to have acoustical impedance matched to that of the air, make granular type materials an optimal choice. The characteristics of this type of materials are governed by a set of microstructural parameters that require equipment not usual in acoustic laboratories as vacuum chambers and cumbersome measurement procedures. In this work, an inverse method to determine these microstructural parameters has been proposed. The method is based on the SA technique that has proven to be robust enough in models with a high number of local minima where the use of local traditional algorithms fails. The method proposed is based on optimizing the residue defined as the absolute difference between a measured absorption curve and the one provided by the CS absorption model.

To assess the goodness of the method, a series of measurements of the non-acoustical quantities have been carried out, which provided a reference for validating the SA results. The proposed method has turn out to be very robust and its operative principle keeps it away to get stuck on one of the great amount of existing local minima. It gives results within the confidence interval of reference. Besides, the results present a very narrow spread.

As a summary, the SA method is a good option for accurately determining the microstructural properties of acoustical materials that are necessary to develop acoustical models of this type of

material, which in turn are essential in noise control and building acoustics conditioning.

Acknowledgements

One of the authors (Elcione Moraes) was sponsored by Banco Santander SA (Brazil) through the Ibero-American Scholarship Program (Grant number 021598/2013) for young teachers and researchers.

References

[1] Beranek LL. Design for acoustics (reprinted from July 1949). Phys Today 2014;67:52–6.
[2] Ingard U. Notes on sound absorption. Maine: Kittery Point. 1999.
[3] Fahy F. Fundamentals of engineering acoustics. San Diego: Academic Press; 2001.
[4] Cox TJ, D'Antonio P. Acoustic absorbers and diffusers. London: Spon Press; 2004.
[5] Arenas JP, Crocker MJ. Recent trends in porous sound-absorbing materials. Sound Vib 2010; July:12–7.
[6] Asdrubali F, Schiavoni S, Horoshenkov KV. A review of sustainable materials for acoustic applications. Build Acoust 2012;19:283–312.
[7] Zabalza Brivián I, Valero Capilla A, Aranda Usón A. Life cycle assessment of building materials: comparative analysis of energy and environmental impacts and evaluation of the eco-efficiency improvement potential. Build Environ 2011;46:1133–40.
[8] Voronina NN, Horoshenkov KV. Acoustic properties of unconsolidated granular mixes. Appl Acoust 2004;65:673–91.
[9] Allard JF, Atalla N. Propagation of sound in porous Media. Chichester: John Wiley & Sons; 2009.
[10] Berengier MC, Stinson MR, Daigle GA, Hamet JF. Porous road pavements: acoustic characterization and propagation effects. J Acoust Soc Am 1997;101:155–62.
[11] Champoux Y, Stinson MR. On acoustical models for sound propagation in rigid frame materials and the influence of shape factors. J Acoust Soc Am 1992;92:1120–31.
[12] Atalla Y, Panneton R. Inverse characterization of the geometrical macroscopic parameters of porous materials. Can Acoust 2000;3:80–1.
[13] Bonfiglio P, Pompoli F. Inversion problems for determining physical parameters of porous materials: overview and comparison between different methods. Acta Acust United AC 2013;99:341–51.
[14] Liu S, Chen W, Zhang Y. Design optimization of porous fibrous material for maximizing absorption of sounds under set frequency bands. Appl Acoust 2014;76:319–28.
[15] Meng H, Xin FX, Lu TJ. Sound absorption optimization of graded semi-open cellular metals by adopting the genetic algorithm method. J Vib Acoust 2014;136. 061007-1-8.
[16] Ruiz H, Cobo P, Jacobsen F. Optimization of multiple-layer microperforated panels by Simulated Annealing. Appl Acoust 2011;72:772–6.
[17] Press WH, Flannery BP, Teukolski SA, Vetterling WT. Combinatorial minimization: method of Simulated Annealing. In: Numerical recipes. Cambridge: Cambridge Press; 1986.
[18] Metropolis N, Rosenbluth AW, Rosenbluth MN, Teller AH, Teller E. Equation of state calculations by fast computing machines. J Chem Phys 1953;21:1087–92.
[19] Kirkpatrick S, Gerlatt CD, Vecchi MP. Optimization by Simulated Annealing. Science 1983;220:671–80.
[20] Cerny V. Thermodynamical approach to the travelling salesman problem: an efficient simulation algorithm. J Optim Theory Appl 1985;45:41–51.
[21] Johnson DL, Plona TJ, Scala C. Tortuosity and acoustic slow waves. Phys Rev Lett 1982;49:1840–4.
[22] Champoux Y, Stinson MR, Daigle GA. Air-based system for the measurement of porosity. J Acoust Soc Am 1991;89:910–6.
[23] Rodrigues CF, Lemos de Sousa MJ. The measurement of coal porosity with different gases. Int J Coal Geology 2002;48:245–51.
[24] Birt EA, Smith RA. A review of NDE methods for porosity measurement in fibre-reinforced polymer composites. Insight – Non-Destructive Test Cond Monit 2004;46:681–6.
[25] Zwikker C, Kosten CW. Sound absorbing materials. New York: Elsevier; 1949.
[26] Brown JS. Connection between formation factor for electrical resistivity and fluid-solid coupling factor in Biot's equations for acoustic waves in fluid-filled porous media. Geophysics 1980;45:1269–75.
[27] Allard JF, Castagnede B, Henry M, Lauriks W. Evaluation of tortuosity in acoustic porous materials saturated by air. Rev Sci Instrum 1994;65:754–5.
[28] ISO 9053. Acoustics – materials for acoustical applications – determination of airflow resistance. 1991.
[29] Bies D-A, Hansen CH. Flow resistance information for acoustical design. Appl Acoust 1980;13:357–91.
[30] ISO 10534-2. Acoustics – Determination of sound absorption coefficient and impedance in impedance tubes – Part 2: Transfer-function method, 1998.
[31] Saltelli A. Making best use of model valuations to compute sensitivity indices. Comput Phys 2002;145:280–97.
[32] Sobol IM. Sensitivity analysis for non-linear mathematical models. Math Model Comput Exp 1993;1:407–14.